International Journal of Adhesion & Adhesives 63 (2015) 137–144

Contents lists available at ScienceDirect

International Journal of Adhesion & Adhesives

journal homepage: www.elsevier.com/locate/ijadhadh

Characterization of an acrylic polymer under hygrothermal aging as an optically clear adhesive for touch screen panels

Cho-Hee Park [a], Seong-Ju Lee [a], Tae-Hyung Lee [a], Hyun-Joong Kim [a,b,*]

[a] Laboratory of Adhesion and Bio-Composites, Program in Environmental Materials Science, Seoul National University, Seoul 151-921, Republic of Korea
[b] Research Institute of Agriculture and Life Sciences, Republic of Korea

ARTICLE INFO

Article history:
Accepted 21 August 2015
Available online 3 September 2015

Keywords:
Touch screen panel (TSP)
Acrylic pressure sensitive adhesive (PSA)
Adhesion performance
Viscoelastic property
Aging
Non-corrosive

ABSTRACT

Optically clear adhesives (OCAs) are key components of touch screen panels (TSPs). It is important that OCAs do not affect the transparent electrodes in TSPs because OCAs are contacted to the transparent electrodes. Therefore, N-vinyl caprolactam (NVC) was incorporated in the composition of an acrylic pressure sensitive adhesive (PSA) with excluding an acidic component to maintain the cohesion for OCA preparation. With increasing amounts of NVC, the tack and peel strength of UV-cured PSA increased, but high amounts of NVC led to decreased peel strength. The UV-cured PSA films were placed in a high temperature and humidity chamber for 8 weeks to investigate the durability and corrosion property under hygrothermal conditions. In this study, the corrosion test method using copper foil was suggested as a simple and economical method and was used to evaluate the effect of NVC on the corrosion property of PSA. This method helped identify suitable OCAs that do not have corrosive property. PSA films containing more than 20 wt% of NVC promoted the corrosion of copper foil under hygrothermal aging conditions. The caprolactam ring was opened by moisture, and the PSA structure morphed into a polar structure during the aging process. This change caused a glass transition shift, an increase in the storage modulus at the rubbery plateau, and an increase in peel strength. The surface free energy of the PSA films also increased due to the increase in the polar property. However, high amounts of NVC caused a decrease in the peel strength after 8 weeks of aging because of increased molecular interactions.

1. Introduction

Touch screen panels (TSPs) are common input tools, the application of which in electronic devices is currently expanding. TSPs comprise a cover window, transparent electrodes, and a display module. These constituents are attached to one another with optically clear adhesives (OCAs). In this study, "optically clear" infers that more than 90% of visible light can transmit through the adhesive. This property is essential for displaying the images passing through each component of the TSP on the display module. Generally, an OCA is contacted on the cover window and transparent electrodes, especially in capacitive-type TSPs (Fig. 1), which are commonly used in recent electronic devices [1]. Therefore, it is important for OCAs not to influence the transparent electrode because the electrode is a key component driving the TSP.

Acrylic adhesives were mostly chosen as OCAs due to their fast UV curability and excellent clarity and economical aspect. These adhesives usually contain an acidic component, which is representative of acrylic acid (AA), to improve the cohesion and supply the remaining reaction site with a curing agent. However, if this acidic component was added to the OCA, it can corrode the transparent electrode contacted to the OCA [2]. Therefore, the acidic component should be excluded from the OCA; however, it is essential to incorporate an alternative material into the OCA to maintain the cohesion.

N-vinyl caprolactam (NVC) can be a good replacement for AA. The nitrogen atom in an NVC structure has high electronegativity; therefore, NVC can help enhance the cohesion of OCAs. NVC has been employed in other studies for medical pressure sensitive adhesives (PSAs) [3,4], self-adhesive products, such as labels [5,6], drug delivery systems [7], and dental materials [8].

Several studies on OCAs have been published. Acrylic OCAs for color filters in liquid crystal displays have been reported by Chang and Holguin. OCAs were applied to color filters and changed to a near-structural adhesive by UV and thermal curing [9]. Titanium oxide [10], hafnium carboxyethyl acrylate [11], and zirconium carboxyethyl acrylate [12] blended acrylic PSAs have also been

* Corresponding author at: Laboratory of Adhesion and Bio-Composites, Program in Environmental Materials Science, Seoul National University, Seoul 151-921, Republic of Korea. Tel.: +82 2 880 4784; fax: +82 2 873 2318.
E-mail address: hjokim@snu.ac.kr (H.-J. Kim).

http://dx.doi.org/10.1016/j.ijadhadh.2015.08.012
0143-7496/

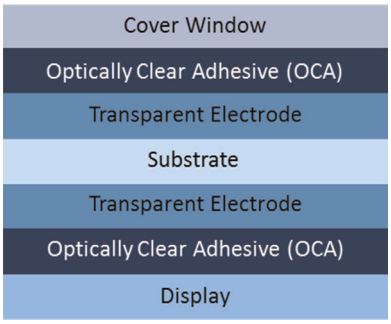

Fig. 1. Capacitive type TSP structure and OCA application.

studied for OCA applications; the main property of those blends being a high refractive index, which can contribute to clearer images on the display. Various companies have applied for several patents on OCA (pressure sensitive adhesive (PSA) type) or optically clear resins (OCRs, liquid resins) [2,13–16].

A more important property of OCAs compared to the refractive index is the anti-corrosion property towards transparent electrodes. The refractive index of a generic acrylic adhesive is adequate to produce a clear image. In addition, the above-mentioned papers studied AA-containing PSAs as OCAs. Therefore, acrylic PSAs without AA and with an anti-corrosion property need to be studied for application in OCAs. Studies on PSAs that do not have an acidic component and on the corrosive property of PSAs toward a substrate, in this case, a transparent electrode (conductive substrate), have not been published. Accordingly, it is necessary to study this topic – acid-free acrylic PSAs and their properties.

The purpose of this research is to characterize an acrylic OCA, with NVC being incorporated in the main polymer backbone, which will protect the transparent electrodes from corrosion by the OCA. Therefore, a PSA-type OCA was prepared with varying amounts of NVC, and its adhesion performance was measured. The durability of the OCA is also important because TSPs will be more widely used in long-term electronic products, such as white goods or automobiles. However, this property has not yet been studied; therefore, the durability of the PSAs prepared in this study should be assessed, as well. Hygrothermal aging is generally used as a test method to determine the suitability of an OCA before any actual application by intentional exposition to a harsh environment. Consequently, the prepared OCA was submitted to property tests including adhesion performance and corrosion property after exposition to hygrothermal aging conditions. Additionally, a method for detecting the corrosive property of PSA toward the transparent electrode was suggested as a simple and economical one.

2. Experimental

2.1. Materials

2-Ethylhexyl acrylate (2-EHA, Samchun Pure Chemical, Republic of Korea), isobornyl acrylate (IBOA, Sigma-Aldrich, USA), and N-vinyl caprolactam (NVC, Sigma-Aldrich, USA) were used to prepare the monomer premix. 1,6-Hexanediol diacrylate (HDDA, Miwon Specialty Chemicals, Republic of Korea) was used as a crosslinking agent. The photoinitiator for the premix preparation and UV-curing was α,α-dimethoxy-α-phenylacetophenone (Irgacure 651, BASF, Germany). All reagents were used without any further purification.

Table 1
Monomer ratio for premix preparation by UV irradiation.

	#1	#2	#3	#4	#5
2-EHA (wt%)	60	60	60	60	60
IBOA (wt%)	40	35	30	20	0
NVC (wt%)	0	5	10	20	40
T_g of cured PSA film (°C)[a]	−40.8	−32.1	−28	−16.6	−22.6

[a] Measured by ARES.

2.2. Monomer premix preparation

A 300 mL round-bottomed flask was equipped with a mechanical stirrer, thermometer and N_2 purging tube. Then, each monomer was charged into the flask, in concentrations given in Table 1. The amount of photoinitiator used was 0.04 phr. Five monomer premixes with different amounts of NVC were prepared by UV-irradiating 2-EHA, IBOA, NVC, and the photoinitiator mixture using a UV-spot cure system (SP-9, USHIO, Japan) of 40 mW/cm^2 intensity under a N_2-rich atmosphere for approximately 3 min. The average viscosity of all the monomer premixes after UV irradiation was approximately 870 cPs, as measured with a Brookfield viscometer using a No. 4 spindle under 750 rpm at room temperature. The molecular weight of each monomer premix was detected by gel permeation chromatography. The monomer premix was diluted with tetrahydrofuran to 1%. The instrument was Agilent 1100 S (USA) and 5-μm polystyrene column was used.

2.3. Coating and curing

Each premix was blended with 0.1 phr of HDDA and 0.15 phr of additional photoinitiator using a paste mixer (Daewha Tech Co. Ltd, Republic of Korea) for 5 min under 1000 rpm. The heat generated during blending was not considered. These mixtures were coated on a PET film for peel strength measurements and the dry-thickness of the coated PSAs was 175 μm. The mixtures were also coated on a release film for viscoelastic property measurements and the dry-thickness of the coated PSAs was 500 μm. The coated samples were UV-cured using conveyor belt type UV-curing equipment with 1000 mJ/cm^2 doses and formed the PSA film after UV-curing.

2.4. Gel fraction

To measure the gel fraction of each sample, the UV-cured PSA films were soaked in toluene for 24 h at 50 °C after weighing each sample. After eliminating the toluene, the swelled PSA films were fully dried for 24 h at 50 °C. After drying, the samples were weighed, and the gel fraction was finally determined. The gel fraction of the cured PSA films was calculated from the following equation.

$$\text{Gel fraction}(\%) = (W_1/W_0) \times 100$$

where W_0 is the initial weight of the sample and W_1 is the solvent extracted weight [17].

2.5. Transmittance

A UV/visible spectrophotometer (Cary 100 UV–vis, Agilent Technologies, USA) was used to evaluate the visible light transmittance of the PSA films used as OCAs in this experiment. The wavelengths of the measurements ranged from 400 to 700 nm. The UV-cured PSA films, which were coated on the PET film, were

loaded on the equipment, and a bare PET film was used for setting the baseline (100% transmittance).

2.6. Tack and peel strength

The probe tack and peel strength were measured with a Texture Analyzer (TA.XT. plus, Stable Micro Systems, UK) at room temperature. The probe was a cylinder with a 5-mm diameter made of stainless steel. The probe was contacted on the surface of the PSA film at a speed of 0.5 mm/s and with a force of 100 g/cm^2 for 1 s. Then, the probe was detached at a speed of 10 mm/s. The maximum force when the probe was detached from the PSA film surface was regarded as the probe tack result. The substrates used in the peel strength test were glass and polycarbonate (PC), which are representative materials for a TSP cover window. A 1-in. wide PSA film was attached to each substrate and was pressed twice by a 2 kg rubber roller. The test speed was 5 mm/s. The peel strength measurements were performed 24 h after preparing the specimens. The peel strength was determined by the average force during the test.

2.7. Aging conditions

The aging conditions for the examination of the durability and corrosion property of the PSA films were 50 °C and 80% relative humidity (RH). The UV-cured PSA films were stored in a conditioned oven for 2, 4, and 8 weeks. After each aging period, each PSA film was assessed in terms of the peel strength, corrosion property, surface property, and viscoelastic property.

2.8. Corrosion test through copper foil color change and resistance increase

The corrosive property of PSA towards transparent electrodes was indirectly tested via the color change of copper foil, which is a simple and economical method. The UV-cured PSA films were deposited on copper foil and stored under the aging conditions mentioned in Section 2.7, for 2, 4, and 8 weeks. The color of the copper foil changed gradually with time. The color of the copper foil was detected by a spectrophotometer (TECHKON SP 820 λ, TECHKON GmbH, Germany). The lightness (L), redness (a), and yellowness (b) values were determined and used to calculate the degree of the color change, ΔE, according to the following equation.

$$\Delta E = \sqrt{(L_1 - L_2)^2 + (a_1 - a_2)^2 + (b_1 - b_2)^2}$$

where, L_1, a_1, and b_1 correspond to data before aging and L_2, a_2, and b_2 correspond to data after each aging period [18].

Moreover, the resistance increase was measured by employing a sputtered indium tin oxide (ITO) transparent electrode on a PET film. The UV-cured PSA films adhered to the ITO film, and the surface resistance was measured using a low resistivity meter (MCP-T610, Mitsubishi Chemical, Japan) before aging and after 2 and 4 weeks of aging for comparison with the copper foil color change test. The measurement point was located close to the PSA attachment. The resistance increase was calculated from the following equation:

$$\text{Resistance increase}(\%) = (R_2 - R_1)/R_1 \times 100$$

where R_1 is the initial surface resistance and R_2 is the surface resistance after the aging period (2 and 4 weeks).

2.9. Viscoelastic property

The viscoelastic property was observed using an advanced rheometric expansion system (ARES, Rheometric Scientific, USA). The test sample contained 20 wt% NVC as a representative example of a PSA film to evaluate the aging behavior in this study. The temperature sweep test was carried out from −50 to 150 °C with a heating rate of 3 °C/min. The frequency was 1 rad/s, and the strain was 1%. A parallel plate accessory with a 25 mm diameter was used for the measurement. The gap between the two parallel plates was 500 μm. The shear storage modulus was plotted as a function of increasing temperature.

2.10. Surface free energy

The surface free energy of the substrate was obtained by measuring contact angles using a contact angle analyzer (Phoenix-10, Surface Electro Optics, Republic of Korea). Distilled water, diiodomethane, and formamide were used to calculate the surface free energy of glass and PC based on the Lewis acid–base theory for contact angles [19,20]. The surface free energy of the PSA film containing 20 wt% NVC as a representative specimen was measured before aging and after 2, 4, and 8 weeks aging.

2.11. X-ray photoelectron spectroscopy (XPS)

The XPS instrument was an Axis-HSI (Kratos Inc., UK) spectrometer equipped with a Mg/Al dual anode, and the X-ray power was 10 mA, 15 kV. The fitting method was a combination of Gaussian and Lorentzian_GL(30) using the casaXPS program for element peak deconvolution. The UV-cured 500 μm PSA film containing 20 wt% NVC was used for the measurement to investigate its alteration after 2 weeks of aging. The C1s spectra were obtained from each individual peak related to the various functional groups that contain carbon atoms.

3. Results and discussion

3.1. UV-cured PSA films as OCAs

All coated samples were UV-cured and formed a PSA film after UV irradiation. In Fig. 2, the gel fraction of the PSA film was very low without NVC. The gel fraction was similar regardless of the amount of NVC after its incorporation. Upon incorporating NVC, the interaction among the molecules was promoted due to the relatively higher polarity of NVC compared to that of the other monomer components. This high polarity is caused by the

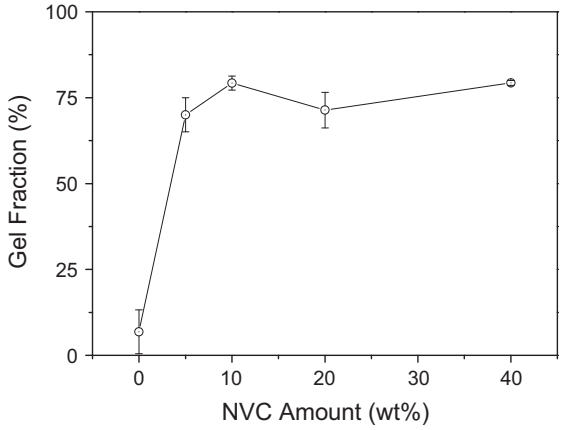

Fig. 2. Gel fraction of the UV-cured PSA films as a function of the amount of NVC.

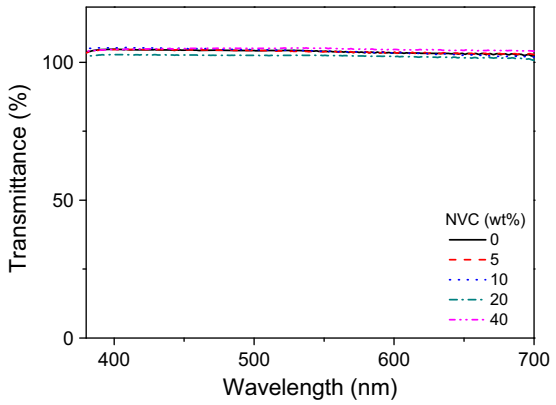

Fig. 3. Visible light transmittance of the UV-cured PSA films deposited on a PET film. (baseline: bare PET film).

nitrogen atom present in NVC. The promoted interaction among the molecules led to a high gel fraction in the UV-cured PSA film. The polarity of NVC affected the cohesion of the UV-cured PSA films [3] and is connected to the adhesion or viscoelastic properties.

The visible light transmittance of the UV-cured films was also approximately 100%; therefore, all prepared samples had excellent clarity and satisfied the optically clear criterion, as shown in Fig. 3. The transmittance calibration was carried out before the measurement using a bare PET film, which is transparent and uncoated. That is, the transmittance value of the bare PET film is 100%. For that reason, the 100% transmittance of the specimen (PSA-coated PET film) implies similar clarity compared to that of the bare PET film. More than 100% of transmittance implies a higher transparency of the PSA-coated PET film than that of the bare PET film. All components were miscible, therefore, the PSA films were achieved without haze.

3.2. Adhesion performance

3.2.1. Tack

Fig. 4(a) shows the tack and fracture energy of the UV-cured PSA films. Fig. 4(b) shows the debonding behavior of the samples during the tack measurement, illustrated as a stress–strain curve. The tack increased with the amount of NVC because of its high polar property that arises from the nitrogen atom in its structure. This polar property increased the cohesion of the PSA. The tack was similar for samples containing between 0 and 5 wt% of NVC. However, the fracture energy increased for the samples containing 5 wt% of NVC because the cohesion of the PSA increased upon incorporating the NVC into the PSA. In Fig. 4(b), more force was required to debond fibrils from the probe surface in the tack measurement of the sample containing 5 wt% of NVC than for the sample without NVC.

This result is related to not only the increase of NVC amount but also the molecular weight of the monomer premix before UV-curing as shown in Table 2. Table 2 represents M_n and M_w of the monomer premixes before UV-curing. The crosslink density of the UV-cured PSA films were also provided. The crosslink density was calculated from the following equation.

$$G = \nu RT$$

where G is the shear modulus of the polymer, ν is the crosslink density, R is the gas constant (8.314 cm^3 MPa K^{-1} mol^{-1}), and T is temperature (K) [21]. The molecular weight of the monomer premixes increased with increasing NVC amount although UV was irradiated during the same time and the viscosity after UV irradiation was similar. NVC amount affected the molecular weight of

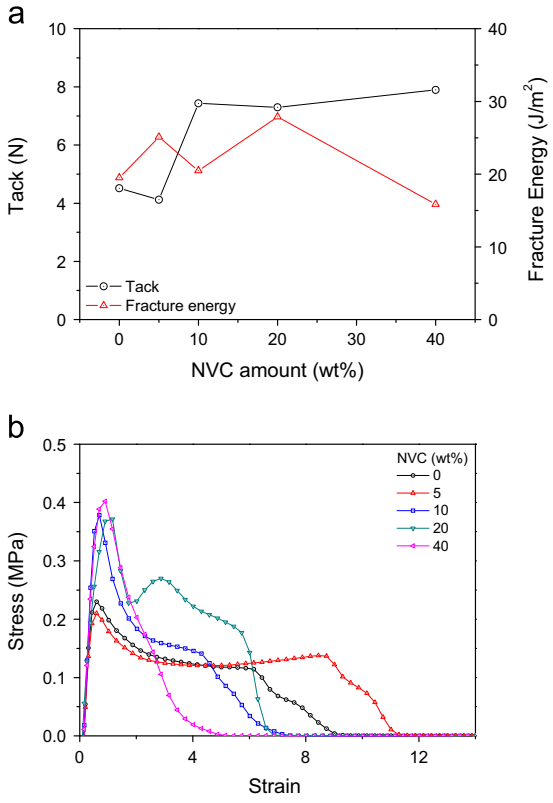

Fig. 4. Probe tack value and fracture energy (a) and stress–strain curve (b) of the UV-cured PSA films as a function of the amount of NVC.

the monomer premix and the crosslink density of the UV-cured PSA film.

Tack values were maintained when incorporating more than 10 wt% of NVC. The fracture energy decreased when the amount of NVC in the PSA was 10 wt% because of elevated tack and decreased fibrillation due to the increased cohesion compared to samples with 0 or 5 wt% of NVC. Then, the fracture energy increased again upon increasing the amount of NVC. The increased intermolecular forces owing to increasing amounts of NVC and the increased entanglement due to the increased molecular weight of the monomer premix led to strong fibrillation. The stress–strain curve shows the largest force required to debond fibrillated PSA from the probe surface for the sample containing 20 wt% of NVC. The second peak in the stress–strain curve supports this result. The fracture energy decreased once more for the sample containing 40 wt% of NVC because of highly increased cohesion among molecules. In this case, fibrillation did not occur.

3.2.2. Peel strength

The peel strength followed a similar trend on both glass and PC, regardless of the substrate, as shown in Fig. 5. The peel strength increased with increasing molecular weight and NVC amount of the monomer premix. This result is related to increased molecular interaction, which is connected to the elevated cohesion of the PSA. Additionally, high molecular weight can give high viscoelastic energy dissipation during debonding due to molecular entanglement [22]. Finally, high peel adhesion of the PSA was accomplished with increasing amounts of NVC. However, the peel strength decreased for the sample containing 40 wt% of NVC because the extremely high cohesion caused a low peel adhesion. This is because high molecular weight and crosslink density brought out restricted molecular mobility. According to this reason, less viscous flow occurred when PSA was bonded to substrate [22].

Table 2
Molecular weight of partially UV-polymerized monomer premixes and crosslinking density of the PSA films after UV-curing.

NVC (wt%)	0	5	10	20	40
M_n (g/mol)	626,500	791,500	1,394,500	1,329,800	2,364,400
M_w (g/mol)	1,322,600	2,087,900	2,809,000	2,705,300	4,186,400
Crosslink density[a] after UV-curing (10^{-3} mol/cc)	0.055	0.061	0.08	0.154	0.245

[a] Calculated from the storage modulus value at rubbery plateau measured by ARES.

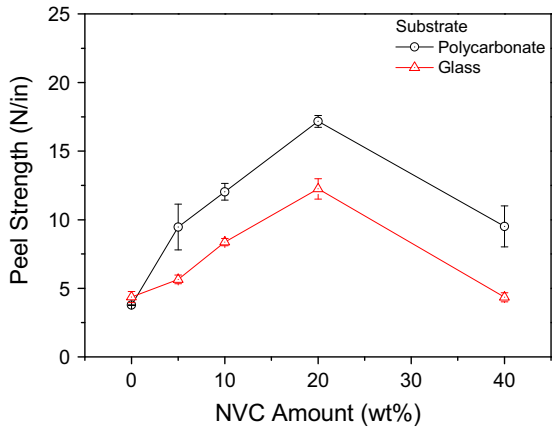

Fig. 5. Peel strength of the UV-cured PSA films with different amounts of NVC.

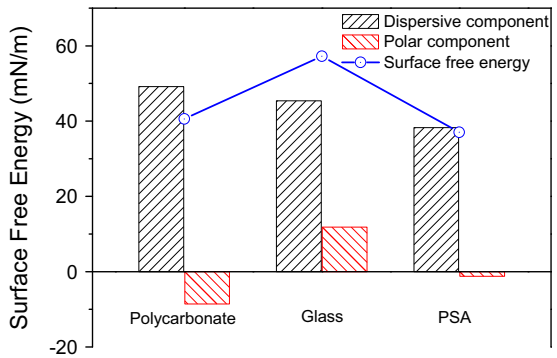

Fig. 6. Surface free energy of the substrates and UV-cured PSA films.

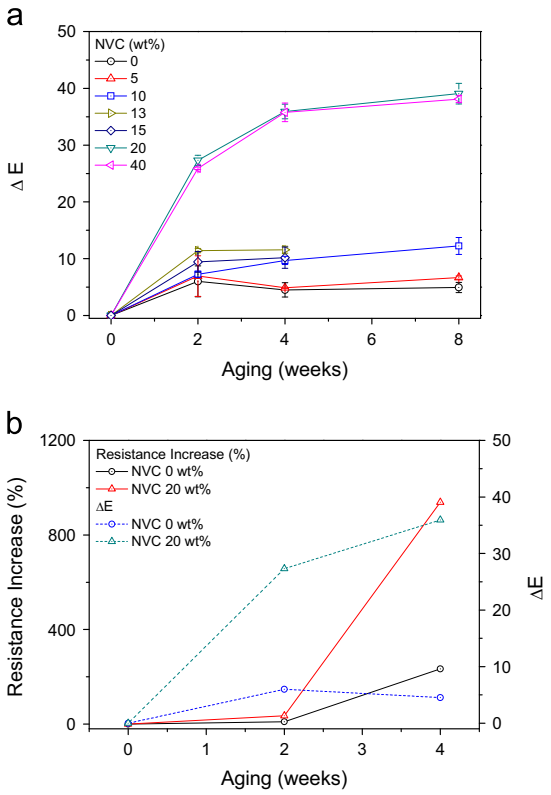

Fig. 7. Copper foil color change due to the UV-cured PSA films (a) and comparison between the resistance increase measurement and the color change (ΔE) (b) under aging conditions.

The difference in the peel adhesion on the two types of substrates arises from the difference in the surface free energy of the two substrates. Fig. 6 illustrates the difference in the surface free energy among 3 types of specimens: PC, glass, and PSA (2-EHA: 60 wt%, IBOA: 20 wt%, NVC: 20 wt%). The peel strength has a high value when the substrate and PSA film have similar surface free energies [23]. The UV-cured PSA film expresses a similar surface free energy compared to PC and a different (lower) surface free energy compared to glass. Accordingly, the peel strength was higher on the PC than on the glass substrate.

Meanwhile, the thermodynamic work of adhesion (W_a) can be obtained from the following equation.

$$W_a = 2\sqrt{\gamma_{SLW(adh)}\gamma_{SLW(sub)}} + 2\sqrt{\gamma^-_{S(adh)}\gamma^+_{S(sub)}}\sqrt{\gamma^+_{S(adh)}\gamma^-_{S(sub)}}$$

The subscripts "adh" and "sub" refer to the adhesive and the substrate, respectively. γ_{SLW} is the dispersive component. γ_s^- and γ_s^+ are the acid and base components, respectively [24]. The calculated W_a of PSA containing 20 wt% of NVC on the glass substrate was 138.98 mN/m and on the PC substrate was 126.74 mN/m. The W_a value corresponds to the amount of work expended to inhibit the interface under reversible or equilibrium conditions. The W_a of the adhesive joints increased with the surface energy of the substrates [24]. The W_a of the PSA on the glass substrate was higher than that on the PC substrate. This trend indicates that more effort was needed to form chemical bonds between the glass substrate and PSA. Therefore, the peel strength on the glass substrate was also lower than that on the PC substrate.

3.3. Aging behavior

3.3.1. Corrosion property

In Fig. 7(a), the change in color of the copper foil upon attaching the UV-cured PSA was monitored for 8 weeks under the aging conditions. More than 20 wt% of NVC affected the severe copper foil color change. However, 5 wt% of NVC did not change the color of the copper foil and thus, the effect of small amounts of NVC on the copper foil was negligible. Moreover, 10 wt% of NVC lead to a slight increase in the ΔE of the copper foil to approximately $\Delta E = 10$. This result implies that, although an acidic component was excluded, an excess amount of polar material might cause latent corrosion via a reaction between PSA and copper in a long-range perspective. More than 20 wt% of NVC turned the copper foil almost black, which corresponds to values of $\Delta E > 25$. This black color is that of copper oxide [25]. The high electronegativity of the nitrogen atom in the NVC structure and that of the carboxyl group formed by the opening of the caprolactam ring facilitated the oxidation of copper under the hygrothermal aging conditions. The caprolactam ring-opening reaction under the

aging conditions will be discussed again in Section 3.3.4. Copper ions were formed by electron loss and reacted with oxygen. Finally, copper oxide was formed, and the color change was observed during the aging process.

The resistance increase of the ITO by PSA adhesion and the ΔE are plotted together in Fig. 7(b). The measurement of the resistance increase was carried out for the first 4 weeks because the ΔE did not change dramatically between 4 and 8 weeks, as shown in Fig. 7(a). The measured samples contained 0 and 20 wt% of NVC. These samples were selected because the difference in ΔE was largest between those samples, whereas the samples containing 5 wt% and 10 wt% of NVC had ΔE values similar to that of the sample without NVC. Moreover, the samples containing 20 wt% and 40 wt% of NVC had similar ΔE values. The ITO resistance increased significantly for 4 weeks, as shown by the ΔE results. The resistance increase of the 20 wt% NVC sample was greater than that of the sample without NVC, which is consistent with the trend in ΔE. The corrosion property of the PSA can be judged early through the copper foil color change test compared to the resistance increase measurement because the ΔE of copper foil showed a sharp increase in comparison with the slower resistance increase of the ITO within 2 weeks. The copper foil color change test can provide information on the PSA corrosion property at an earlier time than the resistance increase measurement.

3.3.2. Viscoelastic property

The glass transition temperature (T_g) was shifted to a higher temperature range, as confirmed by the storage modulus in Fig. 8 and is correlated with restricted molecular mobility. The storage modulus at the rubbery plateau area also increased with the aging time, indicating that a more crosslinked structure was formed [21]. In other words, the shift in T_g and the increase of the storage modulus at the rubbery plateau are related to the increased molecular interaction and crosslinked structure. In this experiment, the increased molecular interaction during the aging process may be due to hydrogen bonding. The structural change of the molecules that construct the PSA occurred under the high temperature and humidity conditions. This molecular change might induce the hydrogen bonding. Thus, a surface free energy analysis and XPS monitoring were carried out to investigate the origin of the viscoelastic property change.

3.3.3. Surface free energy

The surface free energy of the PSA increased with aging time. The increased surface free energy of the PSA is related to the increase in the polar component of the PSA matrix. Fig. 9 shows the surface free energy, which is the sum of the polar component and the dispersive component according to the Lewis acid–base theory. In this graph, the increase in the polar component is clearly observed, implying that the number of polar functional groups increased on the surface of the PSA film; thus, the PSA structure morphed into a polar structure during the aging process. This phenomenon can be related to the shift in T_g of the PSA mentioned in Section 3.3.2, which induced attraction among molecules, as observed in viscoelastic property.

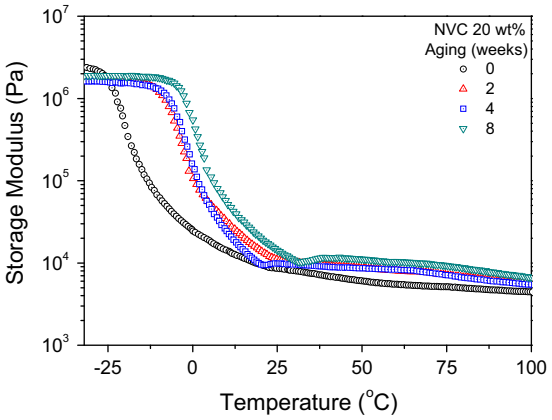

Fig. 8. Shear storage modulus of the aged samples containing 20 wt% of NVC.

3.3.4. XPS spectra

According to Fig. 10, differences in the XPS spectra are observed before and after hygrothermal aging. The viscoelastic property was largely altered after 2 weeks of aging. On that account, the XPS spectra were characterized before and after 2 weeks of aging. After aging, the (C=O)N related peak disappeared [26,27]], and a broad peak related to the O–C=O carboxyl group appeared [28,29]. This substitution reflects the change from the (C=O)N group of the caprolactam ring to an –NH group by reaction under humid

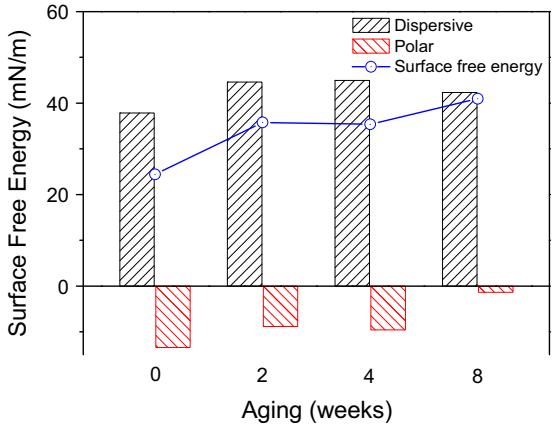

Fig. 9. Surface free energy change of the PSA film containing 20 wt% of NVC during aging.

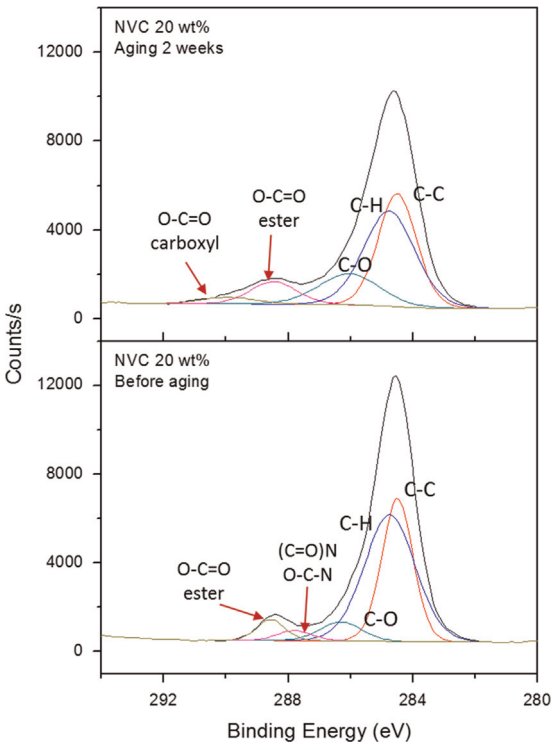

Fig. 10. C1s spectra of the sample containing 20 wt% of NVC before (down) and after (up) aging.

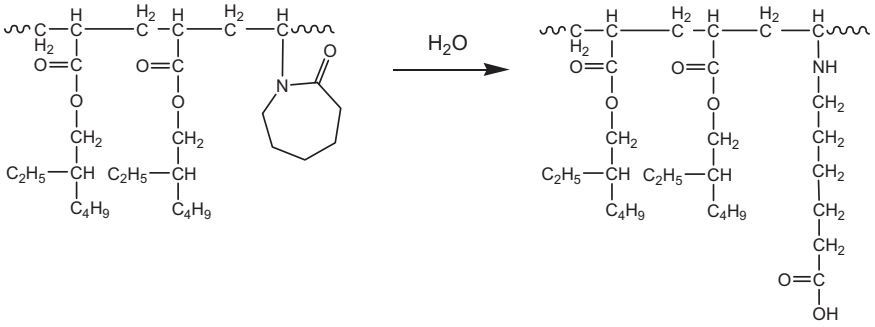

Fig. 11. Schematic diagram of the expected caprolactam ring-opening reaction under humid conditions.

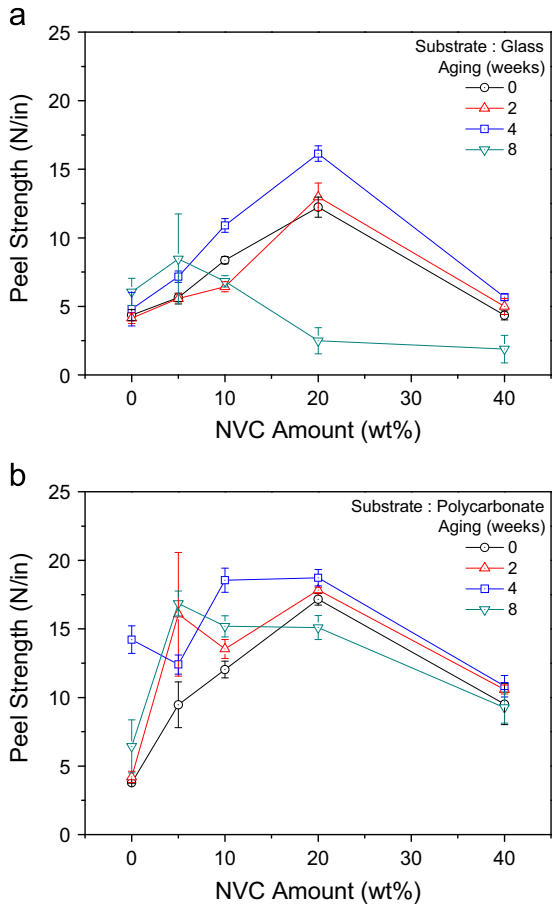

Fig. 12. Peel strength on the glass substrate (a) and on the PC substrate (b) for 8 weeks under aging conditions.

conditions. The carboxyl group was also formed as a result of the caprolactam ring-opening reaction with (C=O)N dissipation. These phenomena contributed to the surface free energy and viscoelastic property change caused by the increase in polar groups. Fig. 11 shows the expected caprolactam ring-opening reaction by moisture corresponding to the XPS results.

3.3.5. *Peel strength*

The change in the peel strength of the samples under the hygrothermal aging conditions is plotted in Fig. 12. The change in peel strength showed similar trends for both substrates, although the numerical value was slightly different. The peel strength increased for the 4 weeks aged samples but decreased for the 8 weeks aged samples, especially for the samples containing 20 and 40 wt% of NVC. This tendency was remarkable on the glass substrate. The increased peel strength during the aging process is due to increased molecular interactions by the formation of –NH and –COOH functional groups by the caprolactam ring-opening reaction, as suggested by the XPS results. These groups are highly polar and can induce hydrogen bonding among other molecules. Hence, the cohesion of the PSA films could increase. However, excessively increased cohesion caused decreased peel strength. Specifically, the decrease in peel strength after 8 weeks of aging can be explained by the large polarity of the glass substrate, as shown in Fig. 5. The –NH and –COOH polar groups in the PSA polymer side chains are more easily oriented toward the glass substrate compared to the PC substrate during the period between the sample preparation and the peel strength measurement. The highly increased intermolecular forces hindered the formation of bonds at the interface between the PSA and the substrate. This increase caused the lower adhesion strength on the glass substrate.

4. Conclusions

NVC was employed to prepare a non-corrosive PSA for application in TSPs, especially when contacted to transparent electrodes to bond each layer. The prepared PSA films exhibited excellent transparency and did not seriously affect the conductive substrate (copper foil) unless more than 20 wt% of NVC was incorporated in the PSA matrix. The corrosion test method of the UV-cured PSA using copper foil was effective because it exhibited an early response, which is the color change of the copper foil, compared to the direct use of a transparent electrode. To examine the stability of UV-cured PSAs under high temperature and humidity conditions, the viscoelastic property was measured. The storage modulus at the rubbery plateau increased, and the T_g was shifted to high temperatures during the aging process because of the increased molecular interactions caused by hydrogen bonding with the polar functional groups. The opened caprolactam ring forms carboxyl groups under humid conditions, which induce hydrogen bonding. Accordingly, the UV-cured PSA films morphed into a more polar structure as well. This result was supported by the surface free energy and XPS measurements. The peel strength of the samples increased until 4 weeks of aging due to the increased polar property of the PSA but decreased after 8 weeks of aging because of the extremely high interaction and cohesion among the molecules. Specifically, samples containing more than 20 wt% of NVC followed that trend.

Acknowledgements

This research was supported by grants from the Lignocellulosic Biomass-based Advanced Eco-materials Technology Team for BK21 PLUS (Project no. 5274-20150100) by the Ministry of Education of Korea.

References

[1] Special adhesives and passivation materials market outlook and application 2012. Fuji Keizai, Tokyo; 2011.
[2] Everaerts AI, Xia J. Indium-tin-oxide compatible optically clear adhesive, United States Patent, 3M Innovative Properties Company, US 2009/0087629 A1; 2009.
[3] Czech Z, Kurzawa R. Acrylic pressure-sensitive adhesive for transdermal drug delivery systems. J Appl Polym Sci 2007;106:2398–404.
[4] Feldstein MM, Bovaldinova KA, Bermesheva EV, Moscalets AP, Dormidontova EE, Grinberg VY, et al. Thermo-switchable pressure-sensitive adhesives based on poly (N-vinyl caprolactam) non-covalently cross-linked by poly (ethylene glycol). Macromolecules 2014;40:5759–67.
[5] Czech Z. Development in the area of UV-crosslinkable solvent-based pressure-sensitive adhesives with excellent shrinkage resistance. Eur Polym J 2004;40:2221–7.
[6] Czech Z. Solvent-based pressure-sensitive adhesives for PVC surfaces: a special report. Adv Polym Technol 2001;20:72–85.
[7] Cespi M, Casettari L, Palmieri GF, Perinelli DR, Bonacucina G. Rheological characterization of polyvinyl caprolactam–polyvinyl acetate–polyethylene glycol graft copolymer (Soluplus®) water dispersions. Colloid Polym Sci 2014;292:235–41.
[8] Moshaverinia A, Chee WW, Brantley WA, Schricker SR. Surface properties and bond strength measurements of N-vinylcaprolactam (NVC)-containing glass-ionomer cements. J Prosthet Dent 2011;105:185–93.
[9] Chang EP, Holguin D. Curable Optically Clear Pressure-Sensitive Adhesives. J Adhes 2005;81:495–508.
[10] Lee S-W, Park J-W, Park C-H, Kwon Y-E, Kim H-J, Kim E-A, et al. Optical properties and UV-curing behaviors of optically clear PSA-TiO_2 nano-composites. Int J Adhes Adhes 2013;44:200–8.
[11] Lee S-W, Park J-W, Park C-H, Kim H-J. Enhanced optical properties and thermal stability of optically clear adhesives. Int J Adhes Adhes 2014;50:93–5.
[12] Kim S, Lee S-W, Lim D-H, Park J-W, Park C-H, Kim H-J. Optical properties and adhesion performance of acrylic PSAs; influence of functionalized monomer and curing agent. J Adhes Sci Technol 2013;27:2265–77.
[13] Everaerts AI, Xia J. Cloud point-resistant adhesives and laminates, United States Patent, 3M Innovative Properties Company, US 8361632 B2; 2013.
[14] Toyama Y, Inoue S, Nagata M, Hosokawa T. Pressure-Sensitive Adhesive Composition for Optical Films, Pressure-Sensitive Adhesive Optical Film and Image Display, United States Patent, Nitto Denko Corporation, US 7862888 B2; 2011.
[15] Katakami E. Photocurable resin composition for laminating optically functional material, Japan Patent, Kyoritsu Chemical Co., LTD., Japan, WO 2010/027041 A1; 2010.
[16] Determan MD, Everaerts AI, Moore CL, Olson DB. High refractive index pressure-sensitive adhesives, United Sates Patent, 3M, USA, US 2010/0048804 A1; 2010.
[17] Park C-H, Lee S-W, Park J-W, Kim H-J. Preparation and characterization of dual curable adhesives containing epoxy and acrylate functionalities. React Funct Polym 2013;73:641–6.
[18] Pfeffer A, Mai C, Militz H. Weathering characteristics of wood treated with water glass, siloxane or DMDHEU. Eur J Wood Wood Prod 2012;70:165–76.
[19] Jaczuk B, Biaopiotrowicz T, Zdziennicka A. Some remarks on the components of the liquid surface free energy. J Colloid Interface Sci 1999;211:96–103.
[20] Wang J, Wang L. The lower surface free energy achievements from ladder polysilsesquioxanes with fluorinated side chains. J Fluor Chem 2006;127:287–90.
[21] Mitra S, Ahire A, Mallik B. Investigation of accelerated aging behaviour of high performance industrial coatings by dynamic mechanical analysis. Prog Org Coat 2014;77:1816–25.
[22] Tobing SD, Klein A. Molecular parameters and their relation to the adhesive performance of acrylic pressure-sensitive adhesives. J Appl Polym Sci 2001;79:2230–44.
[23] Peykova Y, Lebedeva OV, Diethert A, Müller-Buschbaum P, Willenbacher N. Adhesive properties of acrylate copolymers: Effect of the nature of the substrate and copolymer functionality. Int J Adhes Adhes 2012;34:107–16.
[24] Kowalski A, Czech Z, Byczyński Ł. How does the surface free energy influence the tack of acrylic pressure-sensitive adhesives (PSAs)? J Coat Technol Res 2013;10:879–85.
[25] FitzGerald KP, Nairn J, Skennerton G, Atrens A. Atmospheric corrosion of copper and the colour, structure and composition of natural patinas on copper. Corros Sci 2006;48:2480–509.
[26] Walters KB, Hirt DE. Grafting of end-functionalized poly(tert-butyl acrylate) to poly(ethylene-co-acrylic acid) film. Polymer 2006;47:6567–74.
[27] Cheng Z, Teoh S-H. Surface modification of ultra thin poly (ε-caprolactone) films using acrylic acid and collagen. Biomaterials 2004;25:1991–2001.
[28] Wang P, Pan C-Y. Preparation of styrene/acrylic acid copolymer microspheres: polymerization mechanism and carboxyl group distribution. Colloid Polym Sci 2002;280:152–9.
[29] Briggs D, Beamson G. Primary and secondary oxygen-induced C1s binding energy shifts in X-ray photoelectron spectroscopy of polymers. Anal Chem 1992;64:1729–36.